Superheavy Element Studies with TASCA at GSI: Spectroscopy of Element 115 Decay Chains

Rudolph, Dirk

Published in:
JPS Conf. Proc.

DOI:
10.7566/JPSCP.6.010026

2015

Superheavy Element Studies with TASCA at GSI: Spectroscopy of Element 115 Decay Chains

Dirk Rudolph[1], on behalf of the TASCA and TASISpec Collaborations

[1] *Department of Physics, Lund University, Lund, Sweden*

E-mail: Dirk.Rudolph@nuclear.lu.se

(Received August 29, 2014)

Experimental campaigns on investigations of the superheavy elements 115, 117, 119, and 120 were conducted 2011 and 2012 at the gas-filled "TransActinide Separator and Chemistry Apparatus" (TASCA) at the GSI Helmholtzzentrum für Schwerionenforschung, Darmstadt, Germany. Nuclear structure implications of first-ever α-photon coincidence spectroscopy on element 115 and its daughters obtained with the TASISpec set-up are discussed, likewise possible connections between decay chains associated with elements 115 and 117.

KEYWORDS: superheavy elements, actinide targets, gas-filled recoil separator, α-decay chains, X-ray and γ-ray spectroscopy, element 115

1. Introduction

During the past decade, correlated α-decay chains, which all terminate by spontaneous fission, have been observed in several independent experiments using ^{48}Ca-induced fusion-evaporation reactions on radioactive $Z = 92$-98 actinide targets of U, Np, Pu, Am, Cm, Bk, and Cf. The decay chains are interpreted to originate from the production of neutron-rich isotopes with proton numbers up to $Z = 118$ [1]. Major lines of ongoing superheavy element research are:

- The quest for new elements with $Z = 119$ and $Z = 120$.
- The confirmation of anticipated decay chains from elements $Z = 117$ and $Z = 118$.
- Z determination along presumed $Z > 113$ decay chains.
- Single-atom chemistry of $Z \geq 113$ elements and their placement in the Periodic Table of the Elements.

Following successful studies on the synthesis and decay [2,3] as well as the chemistry [4] of flerovium ($Z = 114$), the fusion-evaporation reactions ^{48}Ca + ^{243}Am, ^{48}Ca + ^{249}Bk, ^{50}Ti + ^{249}Bk, and ^{50}Ti + ^{249}Cf were investigated in 2011 and 2012 at the gas-filled separator TASCA at GSI Darmstadt. In several-months long campaigns high sensitivity was reached, especially in the search for element 119. Decay chains of element 117 were observed [5].

Since neither the mass, A, nor the atomic number, Z, of any of these new elements had been measured directly, the TASISpec set-up [6] was employed for high-resolution α, electron, X-ray and γ-ray coincidence spectroscopy. The aim was to observe α-X-ray events to identify uniquely atomic numbers of isotopes along $Z = 115$ decay chains, and to gain nuclear structure insights based on α-γ coincidence measurements [7].

In the following, both generic and specific experimental tools are briefly described. Thereafter, the present status of data analyses and some results from the TASCA campaigns are summarized. In these Proceedings, the focus lies on high-resolution decay spectroscopy of element 115 decay chains.

2. Experimental

Contemporary superheavy element search and spectroscopy experiments rely on four major components, as sketched in Fig. 1(a): a high-intensity heavy-ion accelerator, actinide target foils mounted on rotating wheels, a separator device, and a detection set-up. At the GSI Helmholtzzentrum für Schwerionenforschung the Universal Linear Accelerator (UNILAC) provides pulsed heavy-ion beams (5 ms beam on and 15 ms beam off). At GSI ^{48}Ca and ^{50}Ti beam intensities routinely reach a DC equivalent of about 0.8-1.0 particle μA, which corresponds to 5 to 6 $\times$ 10^{12} ions per second.

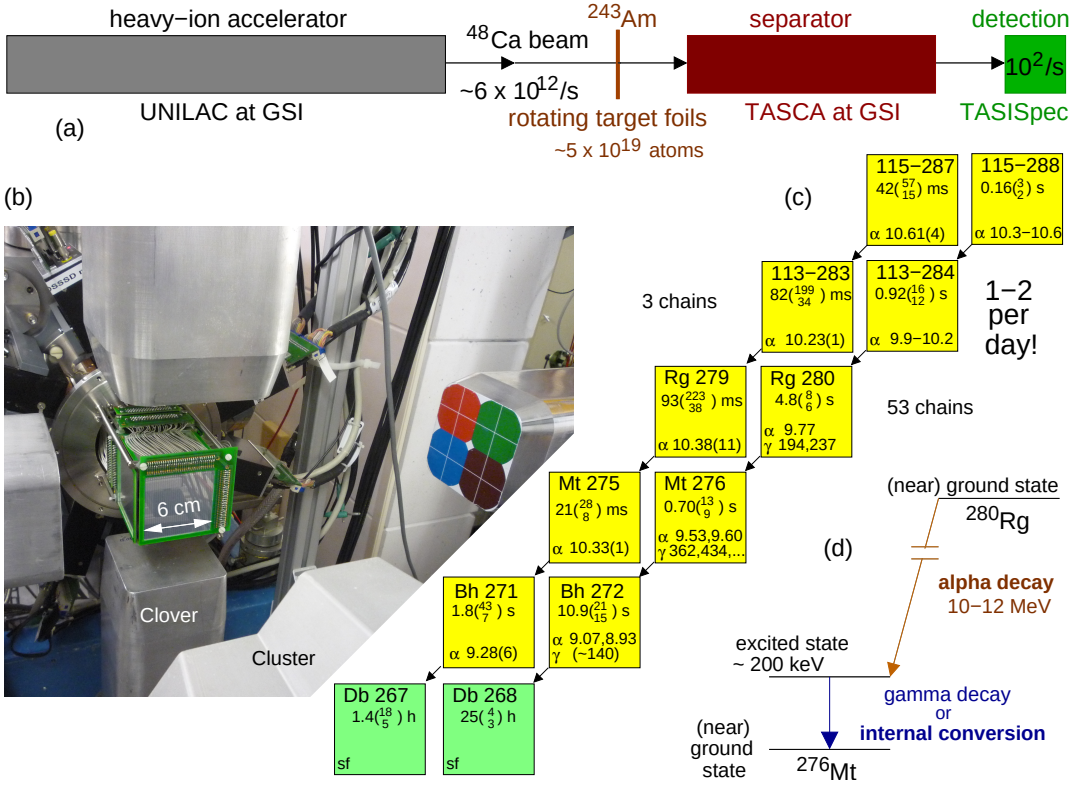

Fig. 1. (a) Sketch of the major components of an experiment to create and study superheavy elements. (b) Photograph of the TASISpec [6] decay spectroscopy set-up in the focal plane of the TASCA. (c) Average decay chains of ^{287,288}115 based on data from FLNR Dubna, Russia, and the TASISpec experiment at GSI [7–9]. (d) Sketch of the idea behind X-ray fingerprinting. Internal conversion decay of excited nuclear states is followed almost always by characteristic K X rays.

To allow for higher beam currents, the transuranium target-wheel system was upgraded in the years 2010 and 2011. The diameter of the wheel was increased to 10 cm holding four arc-shaped target segments with an active area of 6 cm^2 each [10]. The heat load produced by each 5 ms UNILAC beam pulse is thus being dissipated over a considerably larger area than in the earlier configuration, which in turn allows for safe operation with higher primary beam currents. The radioactive actinide target materials are electrodeposited on 2.0-2.2 μm thick Ti backing foils by molecular plating [11]. Typical thicknesses of the deposited actinides are 0.4-0.8 mg/cm^2.

Following extended ion-optical simulations [12, 13] and a number of successful test experiments, a change of philosophy for the focusing scheme of the TASISpec element 115

experiment was taken [14]. Another prerequisite for any successful experiment at gas-filled separators such as TASCA is a reliable assessment of average charge states of superheavy element moving in dilute gas [15] – simply because the best choice of magnetic rigidity, $B\rho$, heavily depends on it.

Next to a recoil transfer chamber aimed for superheavy element chemistry experiments [4, 16], the TASCA focal plane can be equipped with two implantation and decay stations comprising pixelized double-sided silicon strip detectors (DSSSD) as core devices. The system covering the full nominal focal plane area consists of $144 \times 48 \approx 7000$ pixels, each 1 mm $\times$ 1 mm in size. It is preceded by a multi-wire proportional counter, which primarily helps to distinguish between implantation and decay events in the implantation DSSSD during UNILAC beam-on periods. More detailed information on this set-up is or will be provided in Refs. [3, 5, 17]. The other arrangement, TASISpec, is illustrated in Fig. 1(b): to be able to measure photons with high efficiency, the set-up is positioned some 20 cm behind the nominal TASCA focal plane. Its more compact 6 cm $\times$ 6 cm DSSSD gives rise to 1000 pixels. Here, also the four side detectors are pixelized, which is necessary to achieve the overall best possible energy resolution for particle detection [18]. Each of the five DSSSDs of the cube is backed up by one large composite Ge-detector. More details can be found in Refs. [6, 14].

Common for both focal plane detector systems is the (partial) use of fast digital sampling pulse processing of so-called FEBEX type, which was developed by and integrated into the TASCA data acquisition system by the GSI Experiment Electronics Division [19]. The signals of Ge-detectors are handled by commercial Struck 100-MHz, 16-bit sampling ADCs. Within the rather hostile radiation environment, in particular during UNILAC beam-on periods and count rates of up to 100 kHz per crystal, the use of high-performance digital electronics is an absolute must to maintain high-resolution quality in the Ge-detector spectra [20].

3. Results

3.1 Elements 119 and 120

Based on a number of previous superheavy element studies and TASCA (commissioning) experiments (see, for instance, Refs. [1–3, 6, 14, 15]), there are by now rather well-defined guidelines and procedures to properly design and optimize the main parameters of an experiment producing a given isotope of elements 114 to 118. The situation is different for experiments searching for new elements, when some crucial parameters need to be based on extrapolations. For example, elements 119 and 120 are exciting as they will start a new period in the Periodic Table of the Elements, representing the alkali and alkaline earth metal in the 8^{th} period.

The main question concerns the choice of the most promising combination of projectile and target material and, related to that, the compound nucleus excitation energy at which one expects the largest production cross section for a new element. First of all, with ${}_{98}$Cf being the last element that can be isolated and handled in sufficient quantities to serve as target material, the very successful approach based on the doubly-magic beam species ${}^{48}_{20}$Ca is no longer at hand to create elements 119 or 120. Consequently, projectiles with $Z > 20$ have to be employed. Prior to the element 120 experiment at TASCA, attempts were made with the reactions ${}^{64}_{28}$Ni+${}^{238}_{92}$U ($\sim$ 120 days, $\sigma < 90$ fb) and ${}^{54}_{24}$Cr+${}^{248}_{96}$Cm (36 days, $\sigma < 560$ fb) at SHIP at GSI [21] and ${}^{58}_{26}$Fe+${}^{244}_{94}$Pu ($\sim$ 60 days, $\sigma < 400$ fb) at the DGFRS at Dubna [22]. An assessment of two basic arguments, reaction asymmetry and excitation energy at the barrier, favours the reaction ${}^{50}_{22}$Ti+${}^{249}_{98}$Cf. This is reflected by various nuclear reaction calculations (see Ref. [23] and references therein[1]): While the trend of all predictions is the same, i.e. Ti+Cf

[1] Ideas on how to synthesize element 120 have also been put forward by Dr. Sheldon Cooper in season 7,

having the largest and Ni+U the smallest cross section, the absolute values for the preferred reaction Ti+Cf stretch from about 1 pb down to less then 10 fb. Similar considerations suggest the reaction $^{50}_{22}$Ti+$^{249}_{97}$Bk for production of element 119. Technical challenges attached to a long-term high-intensity beam of ^{50}Ti were overcome at GSI, likewise ^{249}Cf and ^{249}Bk made available by the US partners. Together with various improvements of TASCA and its detection systems, this led to search experiments on both element 119 and element 120. The analysis of an unprecedented amount of data is currently in full swing.

3.2 Element 117

Subsequent to the long search for element 119, a five-week control experiment on the synthesis of element 117 was successfully conducted [5]. The reaction ^{48}Ca+^{249}Bk was studied at three different beam energies, and two seven-α-long decay chains were observed, largely consistent with previous reports [24, 25] on element 117. This also proved the integrity of the experimental set-up throughout the long element 119 and 120 searches. In Ref. [5] a hitherto unknown 7.9-MeV α-decay branch in ^{270}Db could be discriminated. It is shown to have a long half-life of $T_{1/2} = 1.0^{+1.9}_{-0.4}$ h, while the relevant rate of α-like events within a broad 6-to-12 MeV energy window is $< 10^{-4}$ s^{-1} per pixel. The ability to time- and position-correlate such long-lived α emitters with implantated nuclei is a major technical achievement, owing mainly to the large number of pixels of the TASCA DSSSD and the reduced rate of unwanted background. In conjunction, this implies a very low implantation rate per pixel, which is the prerequisite for the observation of decays of expectedly increasingly long-lived isotopes of superheavy elements when sailing further to the 'Island of Stability' [26].

3.3 Element 115 Spectroscopy

In November 2012 the extensive TASCA cycle concluded with the three-week TASISpec experiment on element 115 [7]. The spectroscopic results on element 115 decay chains became one of the top ten 'Physics Newsmakers of the Year 2013' selected by the American Physics Society [27], eventually not only triggered by the scientific findings but also by the intriguing facet that 'mysteriously' element 115 is starring in various contemporary computer games.

The idea of fingerprinting the proton number of one of the members of decay chains of superheavy elements such as those shown in Fig. 1(c) is sketched in Fig. 1(d): The α-decay pattern is usually more complex for odd-A or odd-odd nuclei than for even-even nuclei, since the decay usually proceeds to excited states in the daughter nucleus [28]. Furthermore, it is not unlikely that decay chains along the same chain of isotopes may follow different decay paths, depending on the (isomeric) starting level of a given α-decay sequence. In return, there is the possibility to observe X-ray photons in the course of the electromagnetic decays of the excited states in α-decay daughter nuclei, namely in connection with internal conversion. X-ray energies can be predicted with high accuracy since long, also for the heaviest elements (e.g. Ref. [29]). They are characteristic for a given proton, thus atomic number [30]: This was used, for instance, to mark the observation of element 106, rutherfordium [31]. Last but not least, high-resolution α-photon coincidence spectroscopy provides first insights into the nuclear structure of the heaviest atomic nuclei known to mankind today, closing in towards the 'Island of Stability'.

3.3.1 Decay Chains

In the preparatory phase, during the experiment, but especially in the offline data analysis, the focus was on spectroscopic energy resolution for both the TASISpec silicon cube and

episode 6 of 'Big Bang Theory'. Interestingly, Dr. Cooper not only encountered issues with the metric system in his calculations, but also missed out on the most promising reaction, namely Ti+Cf.

the germanium detectors. The determination of pixel-by-pixel deadlayer thicknesses across the silicon detectors may serve as an illustrative detail: This knowledge is necessary to maintain spectroscopic α-decay energy measurements in cases when the α particle left signals in both the implantation and one of the box detectors, so-called reconstructed events [18]. The use of modern sampling electronics is very helpful in the case of silicon detectors – e.g., background reduction, offline software optimization, large dynamic range – while it is essential to maintain (almost) nominal Ge-detector energy resolution in a rather hostile radiation environment, as somewhat detailed in Ref. [20].

In total, 30 correlated α-decay chains associated with the production of different isotopes of element 115 were observed [7, 32], corresponding to an overall production cross section of about 10 pb. The α-decay energies and correlation times measured for 23 (22+1) five-α-long chains are in agreement with 33 (31+2) chains reported earlier [8] for the isotopes ^{288}115 and ^{287}115, respectively. Summarizing the hitherto published data yields the two decay chains presented in Fig. 1(c). In particular the 22+31=53 chains associated with ^{288}115 form a statistically very solid reference [20, 32]. In addition, unprecedented α-photon coincidences provide for the very first time detailed decay schemes along the ^{288}115 chain (see below) as well as two bohrium K X-ray candidates in the 4$^{\text{th}}$-generation decay from Mt into Bh, which are consistent with the production of an isotope of element 115 in the first place [7, 20].

Next to the 23 long chains, there are seven shorter recoil-α-fission (2×) and recoil-α-α-fission (5×) chains of non-random origin in the TASISpec data [32]. The interpretation and assignment of these 'short chains' to a certain isotope of element 115 is not straightforward. The problem is raised in Fig. 2, which shows average values of different selections of decay chains associated with the direct (panels (a)-(c), Refs. [7,8,32]) or indirect (panel (d), Refs. [8, 24, 25]) production of isotopes of element 115.

For reference, panel (a) repeats the first three decay steps of the 53 decay chains *consistently* associated with ^{288}115 [7, 8]. Panel (b) shows the average values of the seven new TASISpec short chains [32]. At first sight, both decay times and the rather broad range of decay energies [33] are consistent with the numbers in panel (a). Therefore, the TASISpec data in itself could readily be explained by interpreting the seven short chains as small spontanous fission branches of ^{284}113 or ^{280}Rg, respectively – or, alternatively, as small EC branches with fast-fissioning even-even daughters ^{284}Cn and ^{280}Ds. So far so good.

In fact, this interpretation would also be consistent with the present interpretion of six-

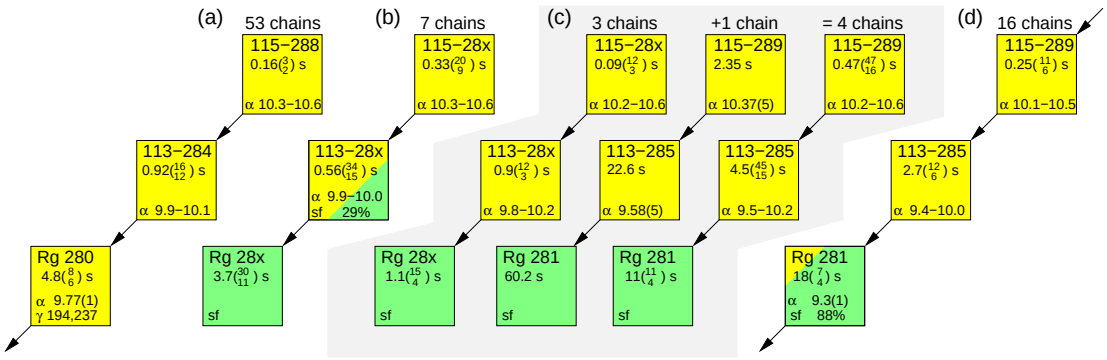

Fig. 2. Average values of different selections of decay chains of isotopes of element 115 into Rg ($Z = 111$) via element 113. (a) ^{288}115 reference chain based on the combination of data from Refs. [7,8] [cf. Fig. 1(c)]. (b) Seven recoil-α-(α) chains observed in the TASISpec experiment [32]. (c) Data from four recoil-α-α 'Dubna chains' listed in Table III of Ref. [8]. (d) Sixteen chains associated with the decay of ^{293}117, i.e. interpreted to populate the isotope ^{289}115 [8, 24, 25].

teen decay chains starting from ^{293}117 [24, 25]. They enter the picture at ^{289}115 [panel (d)]. Especially the decay times of element 113 and Rg isotopes are *different* for chains starting from ^{288}115 in panel (a) [and (b)!], i.e. the chains attributed to ^{293}117 proceed along *different* isotopes – as indeed they should. Still so far so good.

In turn, the element 117 sequence is seemingly compatible with the averages of four recoil-α-α-fission ^{289}115 chains reported and assigned from experiments performed at Dubna [8] and displayed in Fig. 2(c). However, one of these four 'Dubna chains' is quite distinct. Let us decide to separate it from the other three 'Dubna chains', as illustrated in Fig. 2(c) as well: suddenly, these three chains rather match the ^{288}115 reference and the seven 'TASISpec chains' in panels (a) and (b), but certainly *not* the ^{293}117-initiated sequence displayed in panel (d)! Hence, the congruence of decay chains of directly and indirectly produced ^{289}115 as implied in, for instance, Fig. 5 of Ref. [8], hinges primarily on the specific characteristics of just one decay chain, namely chain 3 in Table III of Ref. [8]. Of course, arguments concerning the excitation function of the ^{48}Ca+^{243}Am reaction need to be taken into account as well. More comprehensive considerations and lines of arguments are described in Ref. [32]. Clearly, more high-resolution spectroscopic data is required to solve this puzzling situation.

3.3.2 The E1 Transitions in ^{276}Mt – GEANT4 Consistency Check

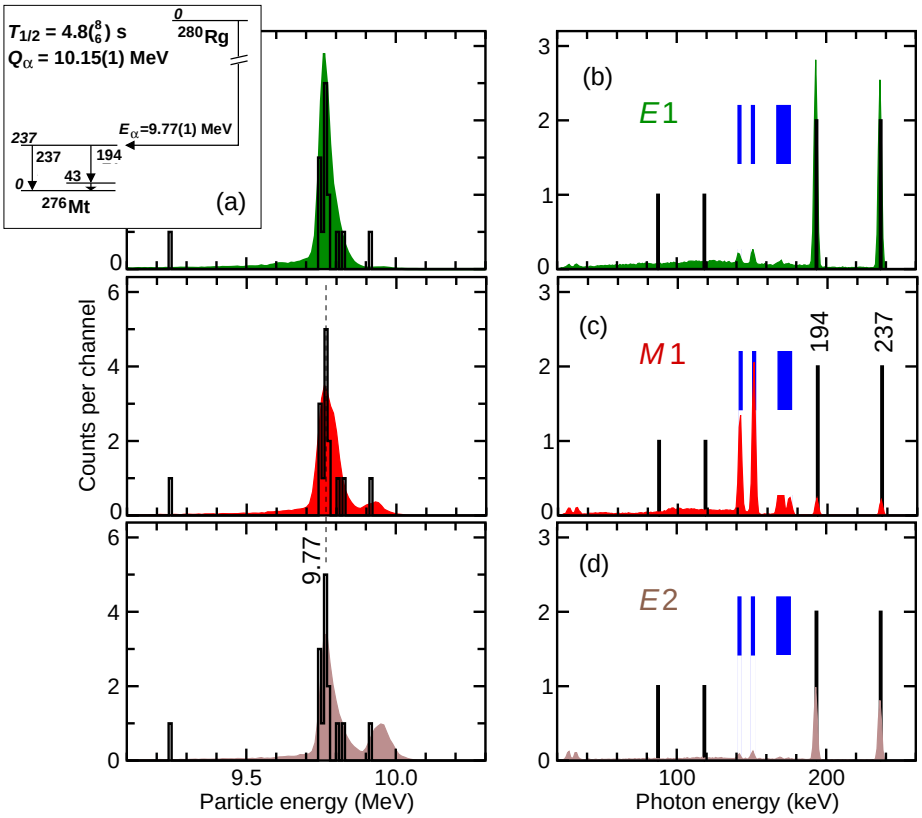

Fig. 3. (a) Decay scheme of ^{280}Rg into ^{276}Mt derived from observed α-photon coincidences [7]. Here, the experimentally observed particle and photon spectra (black histograms) are compared with Geant4 simulations (coloured distributions) assuming different multipole characters for the 194- and 237-keV γ rays [cf. panel (a)]. The vertical blue lines mark K X-ray energies of $Z = 109$, Mt.

The black histograms in Fig. 3(b)-(d) show three times the observed particle and coincident photon spectra of the 3rd-generation decay step of the ^{288}115 chain, namely ^{280}Rg→^{276}Mt. The particle spectrum reveals a rather sharp peak at 9.77(1) MeV, which is interpreted as an α-decay line having that energy. The photon spectrum contains six events; 2×2 counts at 194 and 237 keV, respectively, and two single counts at lower energies. One is tempted to interpret this spectrum as two γ-ray transitions of 194 and 237 keV and two Compton scattered events. Because of inner conversion arguments [34], both γ rays should have electic dipole, $E1$, character. Since the difference 237-194=43 is indicative for an excited rotational level with the same intrinsic structure, the level scheme displayed in Fig. 3(a) follows. But how to add confidence to this nuclear-structure related interpretation, which admittedly is based on scarce data?

The first answer is: perform a self-consistency check with detailed and comprehensive Geant4 simulations of TASISpec and the physics interpretation of the observed data [35,36]! This is exemplified in Fig. 3 by using the decay scheme of panel (a) as Geant4 physics input, but testing three different multipolarities for the 194- and 237-keV γ rays; $E1$, $M1$, or $E2$. The simulations are illustrated by the coloured distributions, normalized to the number of counts in the particle decay spectrum. The yields of the simulated photon spectra on the right hand side are thus a *consequence* of this normalisation, with the efficiency and simulation cross-checked based on known and more abundant α-photon coincidences [36]. The $E1$ interpretation fits in any respect, while $M1$ emission would primarily lead to K X-ray emission with almost no γ-ray yield. $E2$ assignments would imply significant L conversion of the electromagnetic decays, which reduces the yield in the photon spectrum and also leads to a more pronounced bump in the simulated particle spectrum. This bump is due to (partial) summing of α decay and subsequent conversion electron detection in the TASISpec silicon box, all taken care of properly by the Geant4 simulation.

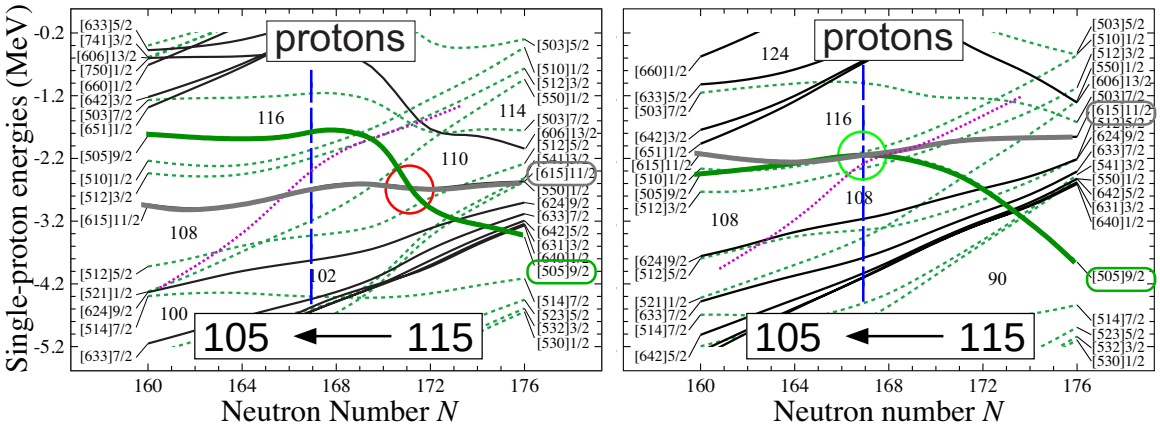

Fig. 4. Proton single-particle energies as a function of neutron number calculated for two different parametrisations of a Skyrme energy density functional: UNEDF1^{SO} (left) and UNEDF1 (right). The underlying diagrams are identical to the lower panels of Figs. 3 and 4 in Ref. [37]. The [615]11/2 (thick grey lines) and [505]9/2 (thick green lines) Nilsson orbitals are highlighted. The long-dashed blue lines denote neutron number $N = 167$ of $Z = 109$ ^{276}Mt. The dotted violet lines mark the Fermi surface along the ^{288}115 decay chain, including ^{276}Mt.

The second answer is: consult contemporary predictions from nuclear structure theory (cf. Ref. [37] and references therein). Available information from purely microscopic as well as microscopic-macroscopic models indicates that roentgenium, meitnerium, and bohrium

isotopes of interest lie in a region of rather stable nuclear quadrupole deformation of $\beta_2 \sim 0.2$ (see, e.g., Refs. [38–42]). Firstly, this 'model-independent' premise is consistent with the new, much more precise experimental Q_α values, which agree very well with predictions concerning the lower part of the $^{288}115$ decay chains [33].

Secondly, it turns out that there are at most two possible explanations amongst Nilsson single-particle states at $\beta \sim 0.2$ for the $E1$ transitions observed in ^{276}Mt: a proton $[615]11/2^+ \rightarrow [505]9/2^-$ or neutron $[716]13/2^- \rightarrow [606]11/2^+$ transition. Moreover, the crossing of the respective two orbitals at or near ^{276}Mt *and* at or near the Fermi surface appears to be the very first *direct* discrimator for any prediction of the shell structure of superheavy nuclei *themselves*. This is exemplified in Fig. 4, which shows the predictions of two different parametrisation of the same recent Skyrme energy density functional for the proton sector [37]: In both descriptions, which differ solely in the spin-orbit strengths, the $[505]9/2^-$ Nilsson orbital approaches the Fermi surface rather quickly. But it is only on the right hand side, where the crossing with the $[615]11/2^+$ Nilsson orbitals occurs for both meitnerium *and* near the Fermi surface (cf. red and green circles in Fig. 4).

Contemporary nuclear structure models should be employed towards nuclear structure based, thus in-depth descriptions of α-decay observables along decay chains of superheavy elements, rather than just comparing global parameters such as Q_α values inferred from nuclear masses. The decay chains of odd-A and odd-odd isotopes are more complex, there are first experiments providing first real decay schemes rather than 'just' chains, and this information requires a more detailed theoretical view as well. See, for example, Refs. [32,33,43] and references therein for more experimental information and first theoretical attempts.

4. Summary

The gas-filled separator TASCA at GSI has reached the forefront of superheavy-element research: For element 115, "... thirty correlated α-decay chains were observed following the reaction ^{48}Ca+^{243}Am. Decay schemes arising from high-resolution spectroscopic coincidence data, in conjunction with comprehensive Monte-Carlo simulations, open the door for direct nuclear structure insights of these heaviest man-made atomic nuclei. Previous assignments linking the majority of the decay chains to the decay of $^{287,288}115$ [8, 9] are confirmed" [7], while the interpretation of short element 115 recoil-α-(α)-fission chains turns out to be more complex. Decay chains from element 117 were confirmed, and search experiments for elements 119 and 120 were conducted with intense ^{50}Ti beams.

Acknowledgements

Personally, I would like to express my gratitude to Ch.E. Düllmann and C. Fahlander for reading the manuscript. On behalf of the TASCA & TASISpec collaborations, I would like to thank the ion-source and the accelerator staff at GSI. We scientists are indebted to technical staff for dedication and action; their expertise is invaluable for the separation of actinide material, target production and target-wheel operation, TASCA operation, slow-control, electronics and data-acquisition, to name but a few. ARIS 2014 attendance and these Proceedings are supported by the Swedish Research Council. The assembly of TASISpec would have been impossible without generous grants from the Royal Physiographic Society in Lund and support from the Euroball Owners Committee. This work is supported by the European Community FP7 – Capacities ENSAR No. 262010, and co-sponsored by the German BMBF, the Helmholtz Society, the Office of Nuclear Physics, U.S. Department of Energy, and the UK Science and Technology Facilities Council.

References

[1] Yu. Ts. Oganessian, J. Phys. G **34**, R165 (2007); Radiochim. Acta **99**, 429 (2011).
[2] Ch.E. Düllmann *et al.*, Phys. Rev. Lett. **104**, 252701 (2010).
[3] J.M. Gates *et al.*, Phys. Rev. C **83**, 054618 (2011).
[4] A. Yakushev *et al.*, Inorg. Chem. **53**, 1624 (2014).
[5] J. Khuyagbaatar *et al.*, Phys. Rev. Lett. **112**, 172501 (2014).
[6] L.-L. Andersson *et al.*, Nucl. Instrum. Meth. A **622**, 164 (2010).
[7] D. Rudolph *et al.*, Phys. Rev. Lett. **111**, 112502 (2013).
[8] Yu. Ts. Oganessian *et al.*, Phys. Rev. C **87**, 014302 (2013).
[9] Yu. Ts. Oganessian *et al.*, Phys. Rev. C **69**, 021601(R) (2004).
[10] E. Jäger *et al.*, J. Radioanal. Nucl. Chem. **299**, 1073 (2014).
[11] J. Runke *et al.*, J. Radioanal. Nucl. Chem. **299**, 1081 (2014).
[12] J.M. Gates *et al.*, GSI Scientific Report 2011, GSI Report 2012-1, PHN-NUSTAR-SHE-14, p. 218.
[13] K.E. Gregorich, Nucl. Instr. Meth. **A711**, 47 (2013).
[14] U. Forsberg *et al.*, Acta Phys. Pol. B**43**, 305 (2012).
[15] J. Khuyagbaatar *et al.*, Nucl. Instr. Meth. **A689**, 40 (2012).
[16] J. Even *et al.*, Nucl. Instr. Meth. **A638**, 157 (2011).
[17] A. Yakushev *et al.*, to be published.
[18] U. Forsberg *et al.*, Eur. Phys. J. Web of Conferences **66**, 02036 (2014).
[19] N. Kurz *et al.*, GSI Scientific Report 2011, GSI Report 2012-1, PHN-IS-EE-02, p. 252; J. Hoffmann *et al.*, ibid., PHN-IS-EE-03, p. 253.
[20] D. Rudolph *et al.*, Acta Phys. Pol. **B45**, 263 (2014).
[21] S. Hofmann *et al.*, GSI Scientific Report 2008, GSI Report 2009-1, NUSTAR-SHE-01, p. 131; GSI Scientific Report 2011, GSI Report 2012-1, PHN-NUSTAR-SHE-01, p. 205.
[22] Yu. Ts. Oganessian *et al.*, Phys. Rev. C **79**, 024603 (2009).
[23] Ch.E. Düllmann, Proc. *5th International Conference on Fission and Properties of Neutron-Rich Nuclei*, 2012, Sanibel Island, Florida, Eds. J.H. Hamilton and A.V. Ramayya, World Scientific, Singapore (2013), p. 271.
[24] Yu. Ts. Oganessian *et al.*, Phys. Rev. Lett. **104**, 142502 (2010).
[25] Yu. Ts. Oganessian *et al.*, Phys. Rev. C **87**, 054621 (2013).
[26] S.G. Nilsson *et al.*, Nucl. Phys. A **131**, 1 (1969).
[27] http://www.aps.org/publications/apsnews/201402/newsmakers.cfm
[28] G.T. Seaborg and W.D. Loveland, *The Elements Beyond Uranium* (Wiley-Interscience, New York, 1990).
[29] T.A. Carlsson *et al.*, Nucl. Phys. **A135**, 57 (1969).
[30] H.G.J. Moseley, Phil. Mag. **26**, 1024 (1913).
[31] C.E. Bemis, Jr. *et al.*, Phys. Rev. Lett. **31**, 647 (1973).
[32] U. Forsberg *et al.*, submitted to Phys. Rev. C.
[33] D. Rudolph *et al.*, J. Radioanal. Nucl. Chem., DOI: 10.1007/s10967-014-3445-y.
[34] T. Kibédi *et al.*, At. Data Nucl. Data Tables **98**, 313 (2012).
[35] L.G. Sarmiento, L.-L. Andersson, D. Rudolph, Nucl. Instrum. Meth. A **667**, 26 (2012).
[36] L.G. Sarmiento *et al.*, Proceedings of Science, PoS(X LASNPA)057 (2014).
[37] Yue Shi *et al.*, Phys. Rev. C **90**, 014308 (2014).
[38] S. Ćwiok, W. Nazarewicz, and P.H. Heenen, Phys. Rev. Lett. **83**, 1108 (1999).
[39] A. Parkhomentko and A. Sobiczewski, Acta Phys. Pol. **B35**, 2447 (2004).
[40] A. Parkhomentko and A. Sobiczewski, Acta Phys. Pol. **B36**, 3115 (2005).
[41] S. Ćwiok, P.H. Heenen, and W. Nazarewicz, Nature **433**, 705 (2005).
[42] I. Ragnarsson, priv. comm.
[43] D.E. Ward, B.G. Carlsson, and S. Åberg, Phys. Rev. C **88**, 064306 (2013).